Inorganic Chemistry

Article

Determination of the Solution Structures of Melamine-Based Bis- and Tris-Macrocyclic Ligand Copper(II) Complexes

Peter Comba,[*,†] **Yaroslav D. Lampeka,**[†,‡] **Alexander I. Prikhod'ko,**[†] **and Gopalan Rajaraman**[†]

Universität Heidelberg, Anorganisch-Chemisches Institut, INF 270, D-69120 Heidelberg, Germany, and L.V. Pisarzhevsky Institute of Physical Chemistry, National Academy of Science of the Ukraine, Prospekt Nauki 31, 02039 Kiev 39, Ukraine

A combination of molecular mechanics (MM), electron paramagnetic resonance spectroscopy (EPR), and spectra simulation (MM–EPR) has been used to determine the solution structures of di- and trinuclear copper(II) complexes of melamine-based oligomacrocyclic ligands. The spin Hamiltonian parameters of the mononuclear, melamine-appended macrocyclic ligand copper(II) complex have been determined by EPR spectroscopy and were also studied with DFT methods. These spin Hamiltonian parameters, together with the structural parameters obtained from models optimized with MM, have been used for the simulation of the EPR spectra of the di- and trinuclear complexes. For the dinuclear complex, the syn isomer is preferred over the anti, for which an X-ray structure exists; for the trinuclear complex, the syn,syn isomer is preferred over the syn,anti form. Additional support for these assignments comes from DFT calculations, and this demonstrates that the MM–DFT–EPR method is a reliable approach for the determination of solution structures and for the analysis of spin Hamiltonian parameters of dipolar, coupled transition metal complexes (**g** and **A** tensors and *J* values).

Introduction

Spectroscopy combined with computational chemistry is a powerful technique for the determination of solution structures and electronic properties of molecular compounds. For paramagnetic metal complexes, EPR spectroscopy is an excellent tool for obtaining structural information that is otherwise inaccessible. The simulation of EPR spectra on the basis of spin Hamiltonian and structural parameters of weakly coupled dinuclear transition metal complexes with $S = 1/2$ each, developed in the 1970s, has been successfully applied to determine solution structures of several dipolar, coupled copper(II) complexes.[1] A more-rigorous approach, which uses a combination of force-field calculations with the simulation of EPR spectra (MM–EPR) was developed a decade ago.[2,3] This eliminates some of the weak points of using only spectra simulations and leads to less ambiguity in the determination of structures of dicopper(II) complexes

in solution. Several examples have been reported in which MM–EPR has been successfully used to access the structural preferences of weakly coupled dicopper(II) complexes in solution.[4–8]

Recently, the syntheses and molecular structures of mono- and oligonuclear copper(II) and nickel(II) complexes with melamine (2,4,6-triamino-1,3,5-triazine)-based macrocyclic ligands have been reported (see Scheme 1).[9–15] Because of the flexible nature of the ligand backbone, the di- and

---

* To whom correspondence should be addressed. Phone: 49-6221-548453. Fax: 49-6226-548453. E-mail: peter.comba@aci.uni-heidelberg.de.
† Universität Heidelberg.
‡ National Academy of Science of the Ukraine.

(1) Simth, T. D.; Pilbow, J. R. *Coord. Chem. Rev.* **1974**, *13*, 173.
(2) Comba, P. *Comments Inorg. Chem.* **1994**, *16*, 133.
(3) Bernhardt, P. V.; Comba, P.; Hambley, T. W.; Massoud, S. S.; Stebler, S. *Inorg. Chem.* **1992**, *31*, 2644.
(4) Comba, P.; Hilfenhaus, P. *J. Chem. Soc., Dalton Trans.* **1995**, 3269.
(5) Comba, P.; Hambley, T. W.; Hilfenhaus, P.; Richens, D. T. *J. Chem. Soc., Dalton Trans.* **1996**, 533.
(6) Comba, P.; Gavrish, S. P.; Hay, R. W.; Hilfenhaus, P.; Lampeka, Y. D.; Lightfoot, P.; Peters, A. *Inorg. Chem.* **1999**, *38*, 1416.
(7) Bernhardt, P. V.; Comba, P.; Fairlie, D. P.; Gahan, L. A.; Hanson, G. R.; Lötzbeyer, L. *Chem.—Eur. J.* **2002**, *8*, 1527.
(8) Comba, P.; Kerscher, M.; Lampeka, Y. D.; Lötzbeyer, L.; Pritzkow, H.; Tsymbal, L. V. *Inorg. Chem.* **2003**, *42*, 3387.
(9) Bernhardt, P. V.; Hayes, E. J. *Inorg. Chem.* **1998**, *37*, 4214.
(10) Bernhardt, P. V.; Hayes, E. J. *J. Chem. Soc., Dalton Trans.* **1998**, 3539.
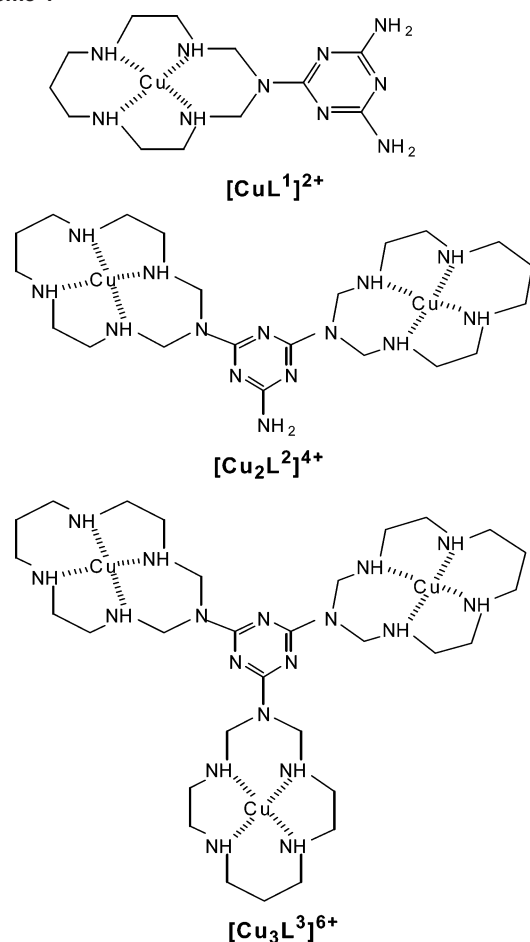(11) Bernhardt, P. V. *Inorg. Chem.* **1999**, *38*, 3481.
(12) Bernhardt, P. V.; Hayes, E. J. *Inorg. Chem.* **2003**, *42*, 1371.
(13) Comba, P.; Lampeka, Y. D.; Nazarenko, A. Y.; Prikhod'ko, A. I.; Pritzkow, H. *Eur. J. Inorg. Chem.* **2002**, 1464.
(14) Comba, P.; Lampeka, Y. D.; Lötzbeyer, L.; Prikhod'ko, A. I. *Eur. J. Inorg. Chem.* **2003**, 34.
(15) Comba, P.; Lampeka, Y. D.; Nazarenko, A. Y.; Prikhod'ko, A. I.; Pritzkow, H.; Taraszewska, J. *Eur. J. Inorg. Chem.* **2002**, 1871.

Scheme 1

$[CuL^1]^{2+}$

$[Cu_2L^2]^{4+}$

$[Cu_3L^3]^{6+}$

Figure 1. Experimental and simulated EPR spectra of $[Cu(L^1)(solvent)_2]^{2+}$.

Table 1. Spin Hamiltonian Parameters of $[Cu(L^1)(OH_2)_2]^{2+}$ Obtained by Simulation of the Experimental Spectrum and by DFT (B3LYP) Calculations (A and a values $\times 10^{-4}$ cm^{-1})

parameter	simulation (exp.)	MM–B3LYP	B3LYP
$g_\perp$	2.041	2.041	2.043
$g_\parallel$	2.191	2.134	2.137
A_x	26.5	−9.7	−7.2
A_y	26.5	−10.1	−11.7
A_z	200.0	−204.4	−197.6
a^{N1}_x		9.0	10.3
a^{N1}_y		9.1	10.4
a^{N1}_z		14.5	15.9
a^{N2}_x		9.0	10.2
a^{N2}_y		9.1	10.3
a^{N2}_z		14.6	15.8
a^{N3}_x		8.5	9.2
a^{N3}_y		8.6	9.2
a^{N3}_z		14.0	14.5
a^{N4}_x		8.5	9.2
a^{N4}_y		8.6	9.3
a^{N4}_z		14.0	14.5

trinuclear complexes, which generally have all copper(II) sites in the expected trans-III configuration, can have several possible conformations, which differ in the relative orientation of the two or three copper sites with respect to each other. Here, we report on the solution structure of the di- and trinuclear copper(II) complexes of L^2 and L^3, established by the MM–EPR method. We also demonstrate that the interpretation of the spin Hamiltonian parameters (J value, **g** and **A** tensors) on the basis of DFT can be combined with the MM–EPR approach (MM–DFT–EPR) to yield additional information and support for the MM–EPR solution structure.

Results and Discussion

Mononuclear Copper(II) Complex. The EPR spectrum of the mononuclear complex $[Cu(L^1)(solvent)_2]^{2+}$ shows the typical features expected for a copper(II) center (Figure 1).[10,14] The region of the perpendicular copper hyperfine lines is partially resolved, but the spectrum does not show any features that can be assigned to superhyperfine interactions due to the nitrogen donors. The simulation of the spectrum (see Figure 1) leads to $g_\perp$ and $g_\parallel$ values of 2.041 and 2.191, respectively, and to copper hyperfine coupling constants ($A_\perp$ and $A_\parallel$) of 26.5 and 200×10^{-4} cm^{-1}, respectively. The determination of the spin Hamiltonian parameters of the mononuclear complex is vital for the simulation of the higher-nuclearity complexes because the individual site
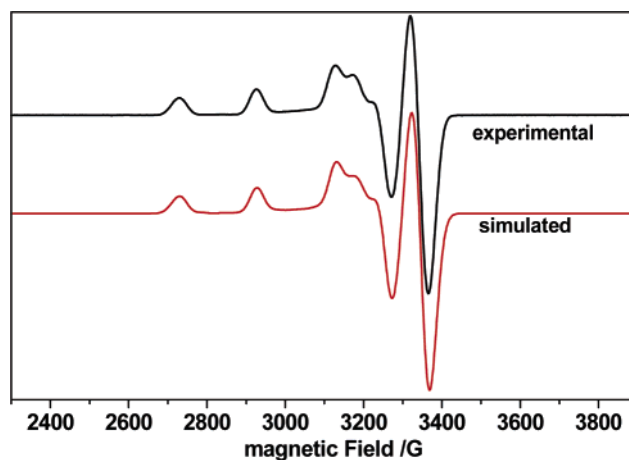
tensors in di- and trinuclear complexes are not expected to deviate much from the mononuclear complex, and such a deviation would question the reliability of the information one can obtain from the present type of simulations.[1]

The spin Hamiltonian parameters discussed here can also be obtained independently and without an experiment by performing DFT calculations. First, the MM-optimized structure was used as an input structure for the optimization of the electronic parameters. Another set of calculations was then performed with a Gaussian-optimized structure.[16] The calculated **g** and **A** tensor values are listed in Table 1. Both sets of DFT-computed parameters are similar, and there is good agreement between the experimental (spectra simulation) and calculated (DFT) values, with the exception of the principle **g** tensor values and the hyperfine values for the perpendicular components (A_x, A_y) of the copper hyperfine interactions. These are underestimated by the DFT calculations, and this is a known effect which generally is believed to be due to the overestimation of covalency in copper(II) complexes by standard DFT functionals ($\Delta g_\parallel$ (exp vs DFT)

(16) The optimization was carried out using B3LYP/6-31G*. The optimization with two axial water molecules did not find a stable minimum, but with only one axial water ligand, a minimum energy structure was found; the frequency calculations indicated that the optimized structure is a true minimum.

of approximately 0.05 is a quite general value).[17−23] A more-accurate estimate of the EPR parameters on the basis of a density functional approach would require a calibration of functionals by an experiment. (see the Supporting Information, Table S1).

The DFT calculations predict a significant superhyperfine interaction with the four nitrogen donor atoms (see Table 1). The calculated superhyperfine values lie in the range $9-10 \times 10^{-4}$ cm^{-1} for the a_x and a_y tensor values, and for the a_z tensor, the values are in the range $14-16 \times 10^{-4}$ cm^{-1}. These parameters do not produce any significant changes in the simulated spectrum and, therefore, a spin Hamiltonian without superhyperfine interactions was used for the simulation of the higher-nuclearity complexes. Classical equations based on ligand field theory[24−29] were used to calculate the spin densities at the copper centers. With the spin Hamiltonian parameters from the EPR spectra simulations, the spin density at the copper center is 0.94 (α^2) with a Fermi contact contribution κ of 0.24. These values are consistent with parameters for other copper(II) tetraamines[30] and indicate that only a small amount of spin density is delocalized to the ligands.

Dinuclear Copper(II) Complex. For the dinuclear complex, several conformations are possible, with the two major minima being the syn and anti conformations (these have the two macrocycles on the same or opposite sides of the melamine plane, respectively; all copper(II) macrocycle geometries were experimentally found and modeled exclusively in the generally most-stable trans-III configuration of the macrocycles). Other possible minima have intermediate conformations related to the rotation of the chromophores around the melamine−macrocycle C−N single bond. For the anti isomer, there is an X-ray structural analysis.[15] However, in solution, the most favorable conformation does not need to be the same as that in the solid.

The MM−EPR method was used for the determination of the conformational preference in solution. The XSophe simulation software[31−33] allows us to construct the molecular
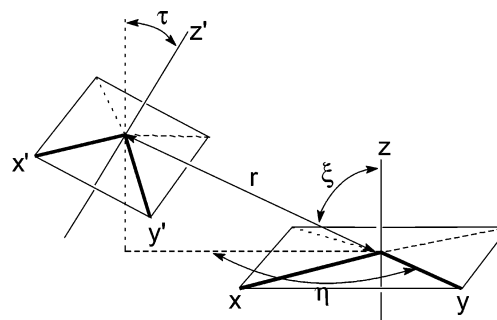
Figure 2. Definition of the structural parameter used in the spin Hamiltonian for the simulation of the EPR spectrum of [Cu$_2$(L^2)(solvent)$_4$]$^{4+}$.
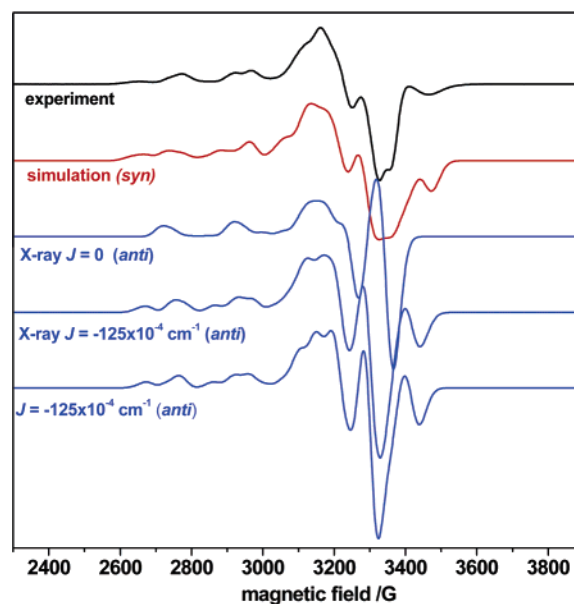
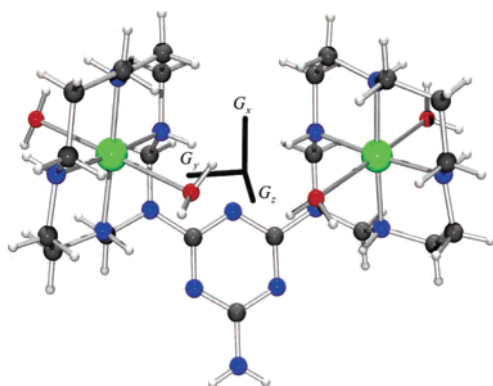**Figure 3.** Experimental and simulated EPR spectra of [Cu$_2$(L^2)-(solvent)$_4$]$^{4+}$. The following parameters were used for the final, optimized simulation: $g_x = g_y = 2.035$, $g_z = 2.191$, $A_x = A_y = 26.5$, $A_z = 210$ ($\times 10^{-4}$ cm^{-1}); $w_x = w_y = w_z = 25 \times 10^{-4}$ cm^{-1} (Gaussian line shape model); $r = 7.0$, $\xi = 30.0$, $\tau = 89.0$ $\eta = 90.0$, $J = -125 \times 10^{-4}$ cm^{-1}.

spin Hamiltonian from the site spin Hamiltonian parameters (**g** and **A** tensor values) together with four structural parameters (r, τ, ξ, and η), which define the relative orientation of the two chromophores (see Figure 2). In general, for dinuclear complexes, the number of variables ranges from 16 (with two different rhombic sets of **g** and **A** tensors for the two chromophores) to 8 (identical sets of **g** and **A** tensors for the two chromophores), without including the exchange-interaction and line-width parameters. Therefore, it is necessary to have a good starting point for the refinement of the spin Hamiltonian parameters. In the present example, the well-defined electronic parameters of the mononuclear complex and the solid-state structural parameters of the dinuclear complex were used as a starting point for the simulation procedure.

The frozen-solution EPR spectrum of [Cu$_2$(L^2)(solvent)$_4$]$^{2+}$ is shown in Figure 3.[14] The spin Hamiltonian for a dipolar, coupled dinuclear complex is given as

$$H = \mu_B B \mathbf{g}_A S_A + I^A \mathbf{A}_A S_A + \mu_B B \mathbf{g}_B S_B + I^B \mathbf{A}_B S_B + J_{AB} S_A S_B + S_A D_{AB} S_B$$

(17) Atanasov, M.; Comba, P.; Martin, B.; Müller, V.; Rajaraman, G.; Rohwer, H. *J. Comput. Chem.* **2006**, accepted.
(18) Neese, F. In *Calculation of NMR and EPR Parameters*; Kaupp, M., Bühl, M., Malkin, V. G., Ed.; Wiley-VCH: Weinheim, Germany, 2004.
(19) Metz, M.; Solomon, E. I. *J. Phys. Chem. A* **2002**, *106*, 2994.
(20) Siegbahn, P. E. M. *J. Comput. Chem.* **2001**, *22*, 1634.
(21) Holthausen, M. C. *J. Comput. Chem.* **2005**, *26*, 1505.
(22) DeBeer George, S.; Basumallick, L.; Szilagyi, R. K.; Randall, D. W.; Hill, M. G.; Nersissian, A. M.; Valentine, J. S.; Hedman, B.; Hodgson, K. O.; Solomon, E. I. *J. Am. Chem. Soc.* **2003**, *125*, 11314.
(23) Neese, F. *Magn. Reson. Chem.* **2004**, *42*, 187.
(24) Gewirth, A. A.; Cohen, S. L.; Schugar, H. J.; Solomon, E. I. *Inorg. Chem.* **1987**, *26*, 1933.
(25) Reinen, D.; Atanasov, M.; Lee, S. *Coord. Chem. Rev.* **1998**, *175*, 91.
(26) Wiersema, A. J.; Windle, J. J. *J. Phys. Chem.* **1964**, *68*, 2316.
(27) Bertrand, P. *Inorg. Chem.* **1993**, *32*, 741.
(28) Atkins, P. W.; Symons, M. C. R. *The Structure of Inorganic Radicals*; Elsevier: Amsterdam, 1967.
(29) Comba, P.; Hambley, T. W.; Hitchman, M. A.; Stratemeier, H. *Inorg. Chem.* **1995**, *34*, 3903.
(30) Hathaway, B. J.; Tomlinson, A. A. G. *Coord. Chem. Rev.* **1970**, *5*, 16.
(31) Wang, D.; Hanson, G. R. *J. Magn. Reson. A* **1995**, *117*, 1.
(32) Wang, D.; Hanson, G. R. *Appl. Magn. Reson.* **1996**, *11*, 401.
(33) Mitchell, A.; Noble, C. J.; Benson, S.; Gates, K. E.; Hanson, G. R. *J. Inorg. Biochem.* **2005**, *96*, 191.

Figure 4. MM model of *syn*-[Cu$_2$(L^2)(OH$_2$)$_4$]$^{4+}$.

Table 2. Structural Parameters from the Crystal Structures and MM Models

structure	Cu···Cu (Å)	ξ (deg)	η (deg)	τ (deg)
X-ray *anti*-[Cu$_2$(L^2)(OH$_2$)$_4$]$^{4+}$ [15]	9.32	10.4	72.1	41.9
MM *syn*-[Cu$_2$(L^2) (OH$_2$)$_4$]$^{4+}$	7.14	42.3	96.5	86.2
MM *anti*-[Cu$_2$(L^2) (OH$_2$)$_4$]$^{4+}$	9.73	4.9	35.8	74.6
EPR [Cu$_2$(L^2) (OH$_2$)$_4$]$^{4+}$	7.00	30.0	95.0	89.0
X-ray *syn,syn*-[Cu$_3$(L^3)(OH$_2$)$_6$]$^{6+}$ [13]				
Cu(1)···Cu(2)	8.50	26.0	15.6	58.8
Cu(1)···Cu(3)	8.50	37.3	10.1	74.6
Cu(2)···Cu(3)	8.00	26.0	15.6	
X-ray *syn,anti*-[Cu$_3$(L^3)(OH$_2$)$_6$]$^{6+}$ [10]				
Cu(1)···Cu(2)	9.50	12.5	21.4	34.3
Cu(1)···Cu(3)	8.00	38.3	7.3	66.2
Cu(2)···Cu(3)	9.40	0.1	21.7	

Table 3. Computed (MM) Structural Parameters and Strain Energies of the Mono-, Di-, and Trinuclear Copper(II) Complexes

complex	strain energy (kJ/mol)	Cu−N (Å)	Cu−Cu (Å)
[Cu(L^1)(H$_2$O)$_2$]$^{2+}$	35.9	2.028	
syn-[Cu$_2$(L^2)(H$_2$O)$_4$]$^{4+}$	48.9	2.030	7.14
anti-[Cu$_2$(L^2)(H$_2$O)$_4$]$^{4+}$	52.7	2.029	9.73
syn,syn-[Cu$_3$(L^3)(H$_2$O)$_6$]$^{6+}$	54.7	2.033	7.18, 7.23, 7.29
syn,anti-[Cu$_3$(L^3)(H$_2$O)$_6$]$^{6+}$	64.4	2.032	9.67, 9.62, 7.25

where g_A, g_B, A_A, and A_B correspond to the individual site **g** and **A** tensors, J_{AB} is the exchange interaction, D_{AB} is the zero field splitting, and S_A and S_B are the spins on the two copper centers ($S_A = S_B = {}^1/_2$). To establish a perturbation treatment, we need all axes to refer to a common coordinate system, and the site B tensor will then be related to that of site A by r_{AB}, (Cu···Cu distance), the polar angles (ξ and η), and Euler angles.

The transition probabilities are strongly dependent on the value of the exchange interaction J_{AB} and the anisotropic exchange. The half-field signal ($\Delta M_S = \pm 2$) has a contribution due only to anisotropic exchange and, therefore, the intensity of this transition decreases with decreasing anisotropic exchange interactions.[34] The relative intensity of the $\Delta M_S = \pm 2$ transitions compared to those with $\Delta M_S = \pm 1$ can be calculated from $I_{rel} = A/r^6_{AB}$, where A is a constant related to the **g** values and the frequency ν of the experiment.

$$A = (19.5 + 10.9\Delta \mathbf{g})\left(\frac{9.100}{\nu}\right)^2$$

With r_{AB} obtained from the MM structure (7.14 Å, see below), the relative intensity of the $\Delta M_S = \pm 2$ transition is 1.6×10^{-4}. This is in agreement with the absence of any feature at half field and indicates that in solution, there are no anisotropic interactions in [Cu$_2$(L^2)(solvent)$_4$]$^{4+}$.

The copper···copper distance (r_{AB}) in the crystal structure is 9.32 Å.[15] Although magnetic exchange between metal ions can be relatively strong, even at such large distances,[35] the propagation through the aliphatic ligand backbone is very weak, i.e., close to zero. Therefore, in a first step of the spectra simulation, the structural parameters from the X-ray structure (Figure 4, Table 2), and the electronic parameters of the mononuclear complex (Figure 1, Table 1) were used. The simulation without magnetic exchange does not give an acceptable fit, specifically, with $J = 0$, the feature at approximately 3450 G is not reproduced. The experimental solid-state magnetic susceptibility data indicate that the two copper ions are antiferromagnetically coupled with $J = -0.45$ cm^{-1} and **g** = 2.17 (see the Supporting Information, Figure S1). Note that the solid-state magnetic susceptibility

is a bulk measurement, on the basis of the response from a sample of randomly oriented molecules in a powder. The magnitude of J is not reliable if J is less than a few wavenumbers. An exchange constant of $J = -125 \times 10^{-4}$ cm^{-1} was necessary to reproduce the feature at 3450 G. However, the structural parameters obtained from the X-ray structure still did not yield an acceptable fit for the EPR spectrum (see Figure 3).

A combination of deterministic and stochastic molecular mechanics searching was therefore used to find structural models for a more-accurate simulation of the spectrum. The two expected conformers, syn and anti with respect to the melamine ring, were found as well-defined minima on the potential-energy surface. The calculated strain energies, the average Cu−N bond lengths, and the Cu···Cu distances for the two isomers are listed in Table 3. The syn isomer, compared to the anti form, is found to be lower in energy by 3.8 kJ/mol. The structure of the anti isomer, calculated by MM, is in good agreement with the X-ray structural data. However, on the basis of the anti structure, there is no acceptable fit for the EPR spectrum. This is different for the computed structure of the syn isomer, which leads to an acceptable fit for the experimental EPR spectrum. A good fit was obtained by modifying some of the structural and spin Hamiltonian parameters of the syn model (see Table 2 and Figure 3 for the structural and electronic parameters and the simulation). The MM optimized syn model is shown in Figure 4. The O···O distance (axially coordinated water) in the syn model is 3.30 Å and suggests a possibility for efficient hydrogen bonding between the two axially coordinated water molecules. Such interactions are expected to be absent in the anti model, where the corresponding O···O distance is 9.80 Å.[15] Note that hydrogen bonding and solvation are not included in our MM model (see the Supporting Information, Figure S3, for the relevant experimental structural background information).

(34) Bencini, A.; Gatteschi, D. *EPR of Exchange Coupled Systems*; Springer-Verlag: Berlin, 1990.
(35) Ruiz, E.; Rodriguez-Fortea, A.; Alvarez, S. *Inorg. Chem.* **2003**, *42*, 4881.

The magnetic exchange interaction between the two copper(II) centers can be calculated with density functional theory methods. The use of B3LYP with an Ahlrich basis set generally gives accurate numerical estimates for J. In the present example, the magnitude of exchange is very small, and it is therefore not possible to obtain a meaningful estimate with DFT. However, the computed J value is useful for understanding how the exchange propagates when the molecule adopts different conformations. The J value calculated on the basis of the anti X-ray structure is $J = -1.0 \times 10^{-3}$ cm^{-1}; on the basis of the MM-optimized syn structure, $J = 0.2$ cm^{-1} (using the $H = -JS_1S_2$ model). The magnitude of J is related to the Cu$\cdots$Cu distance, and as expected for both structures, very small J values are predicted. The exchange interaction propagates through a spin-polarization mechanism (the spin density found on the bridging spacer atoms have alternate signs) rather than a spin-delocalization mechanism. The amount of exchange, which propagates by spin polarization, decreases for structurally related compounds with increasing Cu$\cdots$Cu distance. The shorter Cu$\cdots$Cu distance found for the syn structure (7.14 vs 9.32 Å) is reflected in the calculated magnitude of J. The magnitude of the calculated J value for the syn structure is comparable to the value obtained from the EPR simulations (-125×10^{-4} cm^{-1}) and gives additional support for the proposed solution structure. This indicates that in solution, the Cu$\cdots$Cu distance should be a little shorter than that found in the X-ray structure.

The **g** values for the syn model were calculated by DFT. The **g** tensor is an integral property of the complexes, and the molecular **g** tensor can be related to the site tensor values by the vector coupling approach

$$\mathbf{G} = c_1 g_1 + c_2 g_2$$

where **G** is the molecular **g** tensor, g_1 and g_2 are the site **g** tensor values of the two copper centers, and c_1 and c_2 are the coefficients of the two sites with $c_1 = c_2 = {}^1/_2$. The site **g** tensor values must refer to the same axis system, and the resulting molecular **G** tensor will have off-diagonal elements. Therefore, this matrix needs to be diagonalized to obtain the diagonal elements of the **G** tensor axis. The DFT calculations were performed on the high-spin state of the MM syn model, and this gives $G_x = 2.042$, $G_y = 2.086$, $G_z = 2.092$. These values are in good agreement with those obtained from the experiment (spectra simulation), $G_x = 2.035$, $G_y = 2.113$, $G_z = 2.113$. The principal component of the site tensor value is probably overestimated, and this is reflected in the **G** values as well. Other important information that can be obtained from the DFT calculations includes the orientation of the **G** tensor. The DFT-predicted orientations of the three **G** tensor values are shown in Figure 3. The G_x axis is perpendicular to the Cu$\cdots$Cu bond, and the G_y axis is approximately along the Cu$\cdots$Cu vector. In conclusion, it is shown that the DFT calculations can be combined with the MM–EPR approach (MM–DFT–EPR) to provide additional information and support for the solution structure.

Trinuclear Copper(II) Complex. The approach for the determination of solution structures of weakly coupled
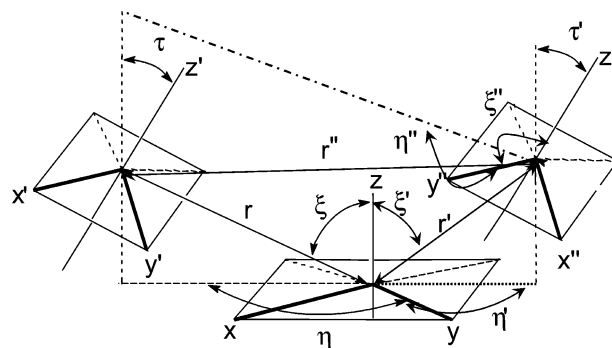
Figure 5. Definition of the structural parameters used in the spin Hamiltonian for the simulation of the EPR spectrum of [Cu$_3$(L^3)(solvent)$_6$]$^{6+}$.
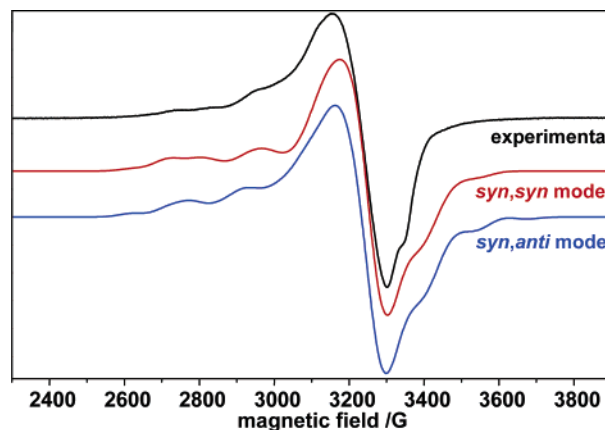
**Figure 6.** Experimental and simulated EPR spectra of [Cu$_3$(L^3)-(solvent)$_6$]$^{6+}$.

trinuclear metal complexes is similar to that for dinuclear complexes. However, the addition of another metal center considerably increases the number of parameters necessary for the simulation (see Figure 5). Although there are several reports on the determination of solution structures of dinuclear complexes, EPR simulations to extract structural information for a trinuclear complex have not been reported before.

The frozen solution (110 K) EPR spectrum of [Cu$_3$(L^3)-(solvent)$_6$]$^{6+}$ at X-band frequency is shown in Figure 6. The crystal structures of two isomers, syn,syn and syn,anti, have been reported.[10,13] From several possible conformations, these two isomers are energetically favored. A preliminary molecular mechanics calculation suggested that the strain energies of the two isomers differ by less than 2 kJ mol^{-1}.[10] The EPR spectrum in solution is not well-resolved. However, some signals in the parallel region are observed around 2700–2900 G.

A solid-state magnetic susceptibility study performed on the powder sample of the syn,syn compound shows that the two copper(II) ions are weakly coupled, and the best fit to the variable-temperature magnetic susceptibility curve is obtained by adopting a spin Hamiltonian model for a single-exchange pathway between the copper centers with $J = -0.48$ cm^{-1} and a **g** value of 2.067 (see the Supporting Information, Figure S2). DFT calculations were also performed on the basis of the two crystal structures (syn,syn; syn,anti) to calculate the exchange interaction between the metal centers. These calculations were performed on different
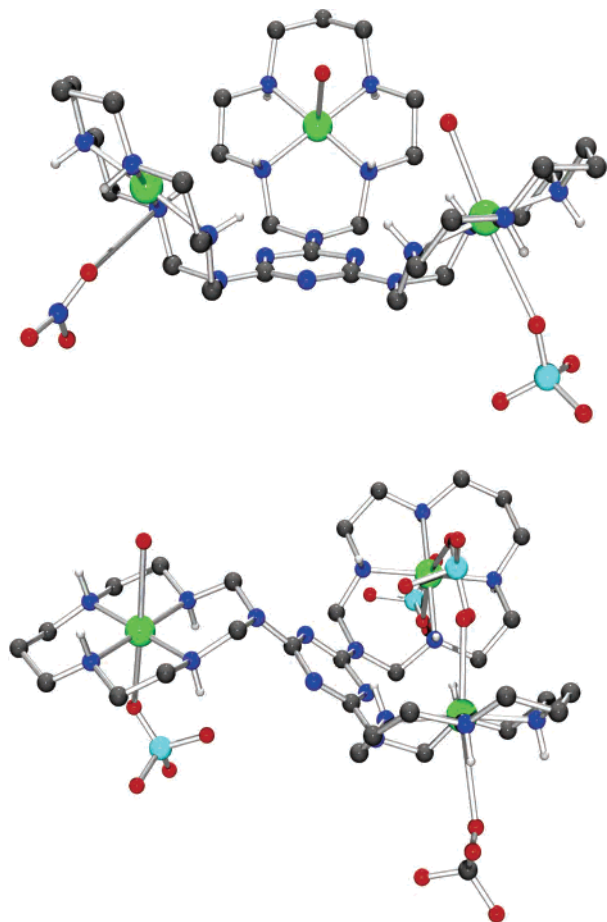
Figure 7. Plots of the experimentally determined molecular structures (X-ray) of the syn,syn and syn,anti isomers of $[Cu_3(L^3)(X)_6]^{n+}$ (X = OH_2, $OClO_3$, ONO_2).[10,13]

spin configurations, and the energy difference between the spin configurations was related to the exchange interactions using the pairwise interaction model.[36,37] For these calculations, a hybrid B3LYP functional was used with an Ahlrich's triple ζ basis set on the copper atoms and a double ζ basis set on all others. Calculations performed on the syn,anti model reveal that the exchange between the copper atom in the anti position with the copper atoms in syn positions (at a Cu···Cu distance of 9.50 Å) is very weak ($J < 1 \times 10^{-3}$ cm^{-1}, see section on the dinuclear complexes for a detailed discussion), compared to the exchange interaction mediated between the two copper atoms in the syn position ($J = -300 \times 10^{-3}$ cm^{-1}, at a Cu···Cu distance of 8.0 Å). With only one exchange pathway for the syn,syn structure, the magnitude of exchange was $J = -1.1 \times 10^{-3}$ cm^{-1}. Note that the Cu···Cu distance in the syn,syn isomer is 8.5 Å and this value is between the distances of 9.50 and 8.0 Å found in the syn,anti model.

The structural parameters of the two isomeric tricopper(II) complexes are given in Table 2. The EPR simulations

performed with the X-ray structural parameters and the spin Hamiltonian parameters of the mononuclear complexes and with the exchange of $J = -125 \times 10^{-4}$ cm^{-1} are shown in Figure 6. Without any modification of the structural and spin Hamiltonian parameter, the syn,syn model gives a much better fit to the experimental spectrum than does the syn,anti model; this indicates that in solution, the syn,syn isomer is favored (see the Supporting Information for a further discussion on details of the EPR spectra and possible implications on the solution structure). The O···O distances of axially coordinated water molecules in the syn,syn isomer are 3.30, 3.32, and 3.35 Å (X-ray data[13]), i.e., at a distance where significant hydrogen bonding is expected, whereas in the syn,anti isomer, these O···O distances are 3.47, 9.08, and 9.13 Å. The larger number of hydrogen bonding interactions in the syn,syn isomer is expected to stabilize the syn,syn isomer in solution.

In conclusion, we have presented the solution structures of dipolar, coupled dinuclear and trinuclear melamine-based oligomacrocyclic ligand complexes using the MM−EPR approach. This method, established for dinuclear complexes, has been adopted and extended to trinuclear complexes. The MM−EPR method reveals that in solution, the syn and syn,syn isomers are preferred over the anti and syn,anti geometries for the di- and trinuclear complexes, respectively. The stabilization of these isomers is believed to be due to hydrogen bonding and (or) ion-pairing effects. Additional support for these structural assignments emerge from DFT calculations. The MM−DFT−EPR approach is therefore suggested for a reliable determination of solution structures and spin Hamiltonian parameters of dipolar, coupled transition-metal complexes.

Experimental Section

General and Measurements. Complexes $[Cu(L^1)(OClO_3)_2]$· H_2O, $[Cu_2(L^2)(OClO_3)_4]$·H_2O·CH_3OH, and $[Cu_3(L^3)(OH_2)_3](NO_3)_3$-$(ClO_4)_3$ were prepared as reported previously.[13] EPR spectra were obtained on frozen solutions with a Bruker ELEXSYS E500 spectrometer (X-band). A mixture of DMF and acetonitrile (volume ratio 2:1) was used as a solvent; the concentration calculated for copper(II) ions was 0.005 mol L^{-1}. The best resolution was obtained at $T = 130$ K by using the modulation amplitude 10 G, time constant 1.28 ms, conventional time 40.96 ms, and sweep time 41.94 ms.

Computational Methods. EPR simulations have been performed with XSophe simulation software,[31,32] and the molecular mechanics calculations were performed with MoMec97[38] with the published force field.[39] The macrocyclic amine nitrogens attached to the melamine ring have been parametrized using the structural features of the mononuclear complex and previously published nitrogen force-field parameters.[39] DFT calculations were performed with the software packages Gaussian03[40] and ORCA.[41] Gaussian03[40] was used for geometry optimizations, the calculation of the exchange interaction on trinuclear complexes, and the computation of frequencies. The ORCA suite of programs was used to calculate the EPR **g** and **A** tensors for the mononuclear complexes and the

(36) Ruiz, E.; Rodriguez-Fortea, A.; Cano, J.; Alvarez, S.; Alemany, P. *J. Comput. Chem.* **2003**, 982.

(37) Ruiz, E.; Alvarez, S.; Rodriguez-Fortea, A.; Alemany, P.; Pouillon, Y.; Massobrio, C. In *Magnetism: Molecules to Materials II*; Miller, J. S., Drillon, M., Ed.; Wiley-VCH: Weinheim, Germany, 2001; Vol. II.

(38) Comba, P.; Hambley, T. W.; Okon, N.; Lauer, G. *MOMEC97, A Molecular Modeling Package for Inorganic Compounds*; University of Heidelberg: Heidelberg, Germany, 1997.

(39) Bernhardt, P. V.; Comba, P. *Inorg. Chem.* **1992**, *31*, 2638.

J constant for the dinuclear complexes. For calculations using ORCA, an Ahlrichs triple ζ basis set with an additional polarization function on Cu;[42] a triple ζ basis set on N, Cl, C, and O; and a double ζ basis set with additional polarization on H were used. To obtain a good estimate of the EPR parameters, we used the flexible CP(PPP) basis set for Cu.[43,44] EPR properties were predicted by coupled, perturbed Kohn−Sham theory for the **g** tensor and the spin−orbit coupling contribution to the hyperfine coupling tensor.[45,46] Fermi contact terms and spin-dipole contributions were obtained as expectation values from the ground-state spin density.

Supporting Information Available: Magnetic data of [Cu$_2$(L^2)-(solvent)$_4$]$^{4+}$ and [Cu$_3$(L^3)(solvent)$_6$]$^{6+}$, EPR spectra in another solvent mixture, a structural plot for the visualization of the H-bonding, and parameters based on DFT calculations with a nonstandard functional (pdf). This material is available free of charge via the Internet at http://pubs.acs.org.

IC052124O

(40) Frisch, M. J.; Trucks, G. W.; Schlegel, H. B.; Scuseria, G. E.; Robb, M. A.; Cheeseman, J. R.; Montgomery, J. A., Jr.; Vreven, T.; Kudin, K. N.; Burant, J. C.; Millam, J. M.; Iyengar, S. S.; Tomasi, J.; Barone, V.; Mennucci, B.; Cossi, M.; Scalmani, G.; Rega, N.; Petersson, G. A.; Nakatsuji, H.; Hada, M.; Ehara, M.; Toyota, K.; Fukuda, R.; Hasegawa, J.; Ishida, M.; Nakajima, T.; Honda, Y.; Kitao, O.; Nakai, H.; Klene, M.; Li, X.; Knox, J. E.; Hratchian, H. P.; Cross, J. B.; Bakken, V.; Adamo, C.; Jaramillo, J.; Gomperts, R.; Stratmann, R. E.; Yazyev, O.; Austin, A.; Cammi, R.; Pomelli, C.; Ochterski, J. W.; Ayala, P. Y.; Morokuma, K.; Voth, G. A.; Salvador, P.; Dannenberg, J. J.; Zakrzewski, V. G.; Dapprich, S.; Daniels, A. D.; Strain, M. C.; Farkas, O.; Malick, D. K.; Rabuck, A. D.; Raghavachari, K.; Foresman, J. B.; Ortiz, J. V.; Cui, Q.; Baboul, A. G.; Clifford, S.; Cioslowski, J.; Stefanov, B. B.; Liu, G.; Liashenko, A.; Piskorz, P.; Komaromi, I.; Martin, R. L.; Fox, D. J.; Keith, T.; Al-Laham, M. A.; Peng, C. Y.; Nanayakkara, A.; Challacombe, M.; Gill, P. M. W.; Johnson, B.; Chen, W.; Wong, M. W.; Gonzalez, C.; Pople, J. A. *Gaussian03,* revision B.03; Gaussian Inc.: Wallingford, CT, 2004.

(41) Neese, F. *ORCA, an ab initio, Density Functional and Semiempirical Program Package*, version 2.4; Max-Planck-Institut für Bioanorganische Chemie: Mülheim an der Ruhr, Germany, 2005.

(42) Schaefer, A.; Horn, H.; Ahlrichs, R. *J. Chem. Phys.* **1992**, *97*, 2571.

(43) The Ahlrichs (2d2fg, 3p2df) polarization functions were obtained from the TurboMole basis set library under ftp.chemi.uni-karlsruhe.de/pub/basen. Sc−Zn: 2p functions from Watchers30 plus one f-function from the TurboMole library.

(44) The ORCA basis set CoreProp was used. This is based on the TurboMole DZ basis developed by Ahlrichs and co-workers and obtained from the basis set library under ftp.chemie.uni-karlsruhe.de/pub/basen.

(45) Neese, F. *J. Chem. Phys.* **2001**, *115*, 11080.

(46) Sinnecker, S.; Neese, F.; Noodleman, L.; Lubitz, W. *J. Am. Chem. Soc.* **2004**, *126*, 2613.